Cell Reports Medicine, Volume *2*

Supplemental information

Longitudinal analysis of humoral immunity against SARS-CoV-2 Spike in convalescent individuals up to 8 months post-symptom onset

Sai Priya Anand, Jérémie Prévost, Manon Nayrac, Guillaume Beaudoin-Bussières, Mehdi Benlarbi, Romain Gasser, Nathalie Brassard, Annemarie Laumaea, Shang Yu Gong, Catherine Bourassa, Elsa Brunet-Ratnasingham, Halima Medjahed, Gabrielle Gendron-Lepage, Guillaume Goyette, Laurie Gokool, Chantal Morrisseau, Philippe Bégin, Valérie Martel-Laferrière, Cécile Tremblay, Jonathan Richard, Renée Bazin, Ralf Duerr, Daniel E. Kaufmann, and Andrés Finzi

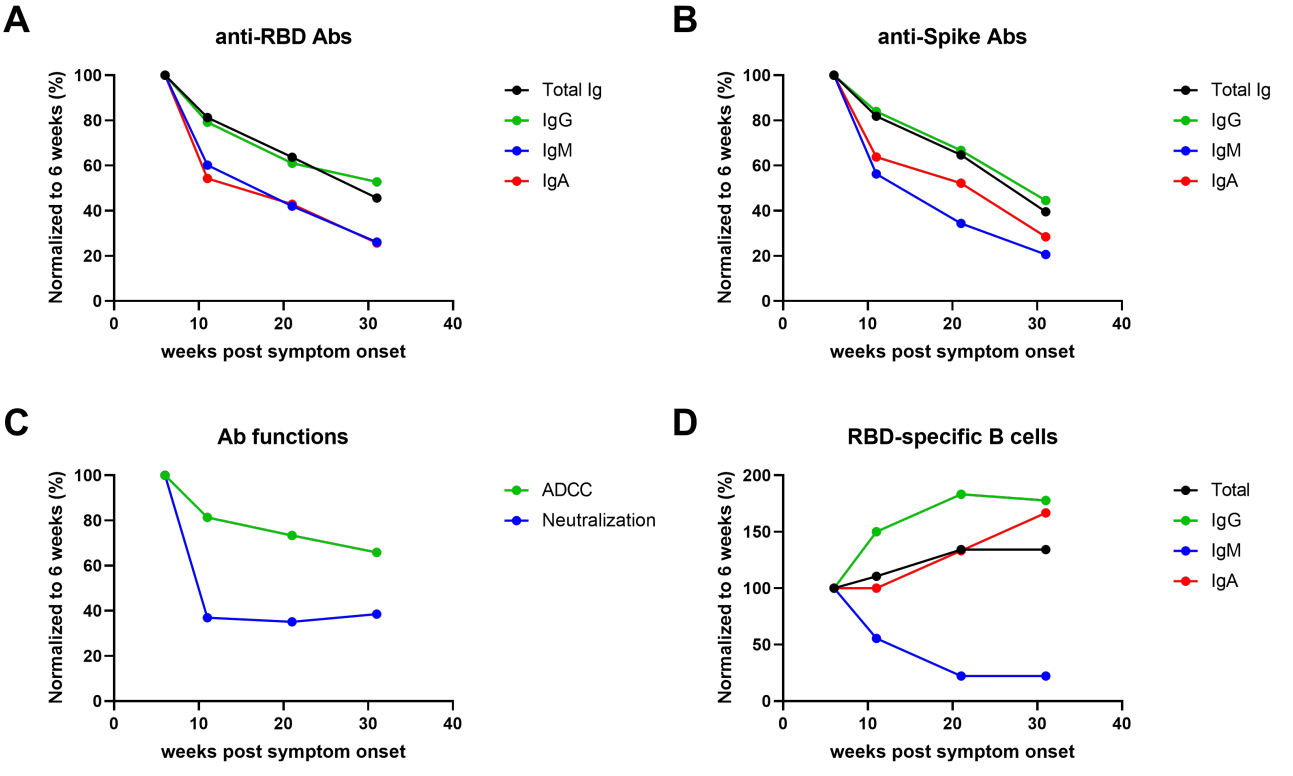

Supplemental Figure 1. Anti-SARS-CoV-2 IgM and IgA levels decline faster than IgG in the convalescence phase - Related to Figure 1, 2 & 3.

(A) The graph shown represents the mean values for anti-RBD ELISA (from Figure 1A-D) at different timepoints (6, 11, 21 and 31 weeks) normalized to the 6 weeks timepoint. (B) The graph shown represents the mean values for anti-Spike cell-based ELISA (from Figure 1E-H) at different timepoints (6, 11, 21 and 31 weeks) normalized to the 6 weeks timepoint. (C) The graph shown represents the mean values for neutralization and ADCC responses (from Figure 2) at different timepoints (6, 11, 21 and 31 weeks) normalized to the 6 weeks timepoint. (D) The graph shown represents the mean values for RBD-specific B cell frequencies (from Figure 3B-E) at different timepoints (6, 11, 21 and 31 weeks) normalized to the 6 weeks timepoint.

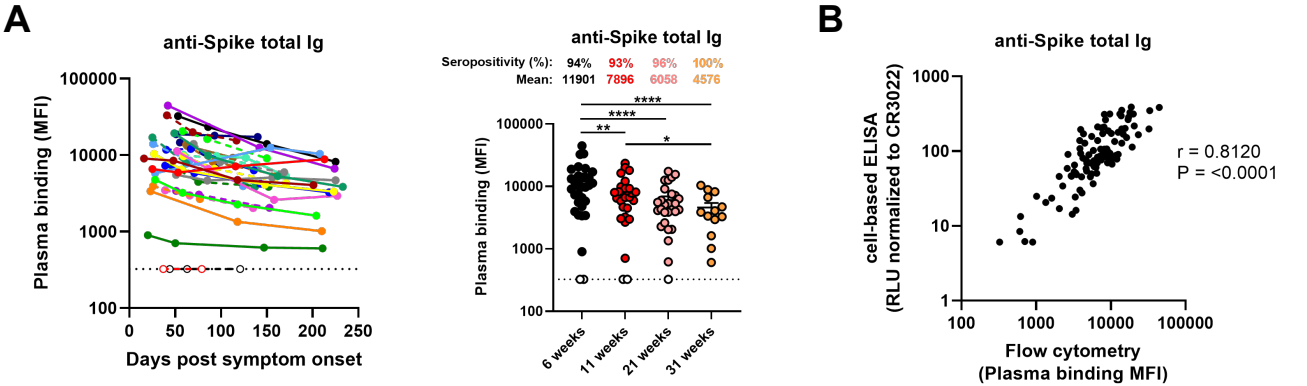

Supplemental Figure 2. Detection of antibodies against SARS-CoV-2 Spike by flow cytometry correlates with anti-Spike detection by cell-based ELISA - Related to Figure 1.

(A) Cell-surface staining of 293T cells stably expressing full-length SARS-CoV-2 Spike using samples from COVID-19+ convalescent donors at different times after symptoms onset (6, 11, 21 and 31 weeks). The graphs shown represent the median fluorescence intensities (MFI) obtained on the GFP+ population. MFIs values obtained with parental 293T (GFP-) were subtracted. (Left panel) Each curve represents the MFIs obtained with the plasma of one donor at every donation as a function of the days after symptom onset. (Right panel) Plasma samples were grouped in different timepoints post-symptom onset (6, 11, 21 and 31 weeks). Undetectable measures are represented as white symbols, and limits of detection are plotted. Error bars indicate means ± SEM. (B) The levels of anti-Spike total Ig quantified by flow cytometry were correlated with the level of anti-Spike total Ig quantified by cell-based ELISA. Statistical significance was tested using (A) a repeated measures one-way ANOVA with a Holm-Sidak post-test or (B) a Spearman correlation rank test (* $P < 0.05$; ** $P < 0.01$; **** $P < 0.0001$).

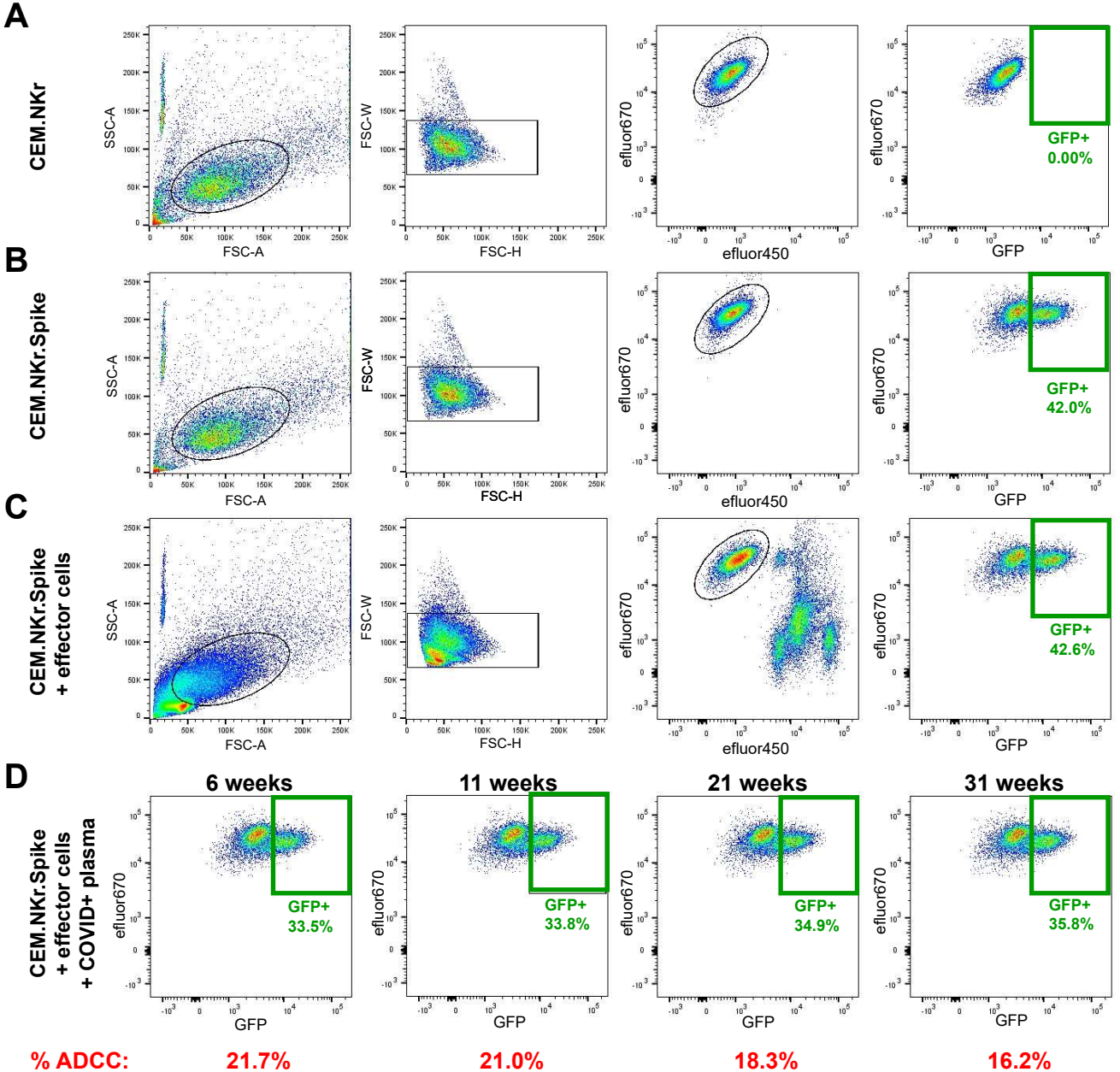

Supplemental Figure 3. Gating strategy for ADCC measurements - Related to Figure 2.
Target cells were identified according to cell morphology by light-scatter parameters (first column) and excluding doublets cells (second column). Cells were then gated on eFluor670+ cells (excluding the effector cells labeled with eFluor450; third column). Finally, the percentage of GFP+ target cells was used to calculate ADCC activity (last column). Examples of gating using (A) parental CEM.NKr or (B) a 1:1 ratio mix of CEM.NKr and CEM.NKr.Spike as target cells in absence or (C) in presence of effector cells. (D) ADCC assay performed in the presence of plasma samples from one representative convalescent donor at 4 different timepoints post-symptom onset (6, 11, 21 and 31 weeks).

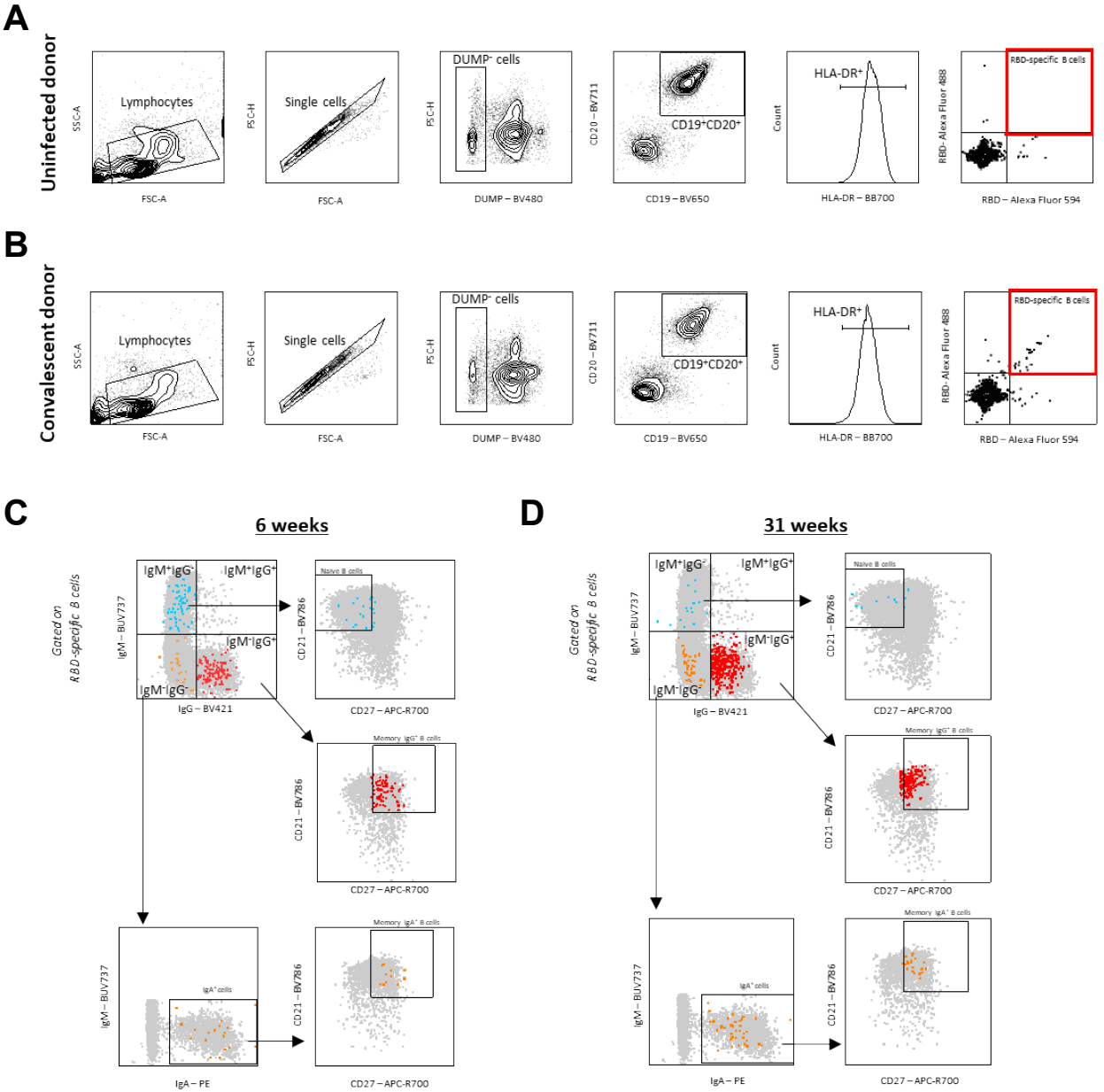

Supplemental Figure 4. Gating strategy for SARS-CoV-2-specific B cell characterization - Related to Figure 3. (A-B) Representative flow cytometry gates to identify RBD-specific B cells from PBMCs of (A) uninfected and (B) convalescent donor. (C-D) Flow cytometry gates used to differentiate RBD-specific B cell subtypes using isotypic and maturation cell surface markers on samples obtained (C) 6 weeks and (D) 31 weeks post-symptom onset. After identification of isotypic subtypes, RBD-specific naïve and memory B cells were characterized based on surface expression of CD21 and CD27. The different RBD-specific B cell subpopulations were superimposed on total CD19+/CD20+/HLA-DR+ B cells (grey). Legend: IgM+ and naïve IgM+ B cells, blue; IgG+ and memory IgG+ B cells, red; IgA+ and memory IgA+ B cells, orange.

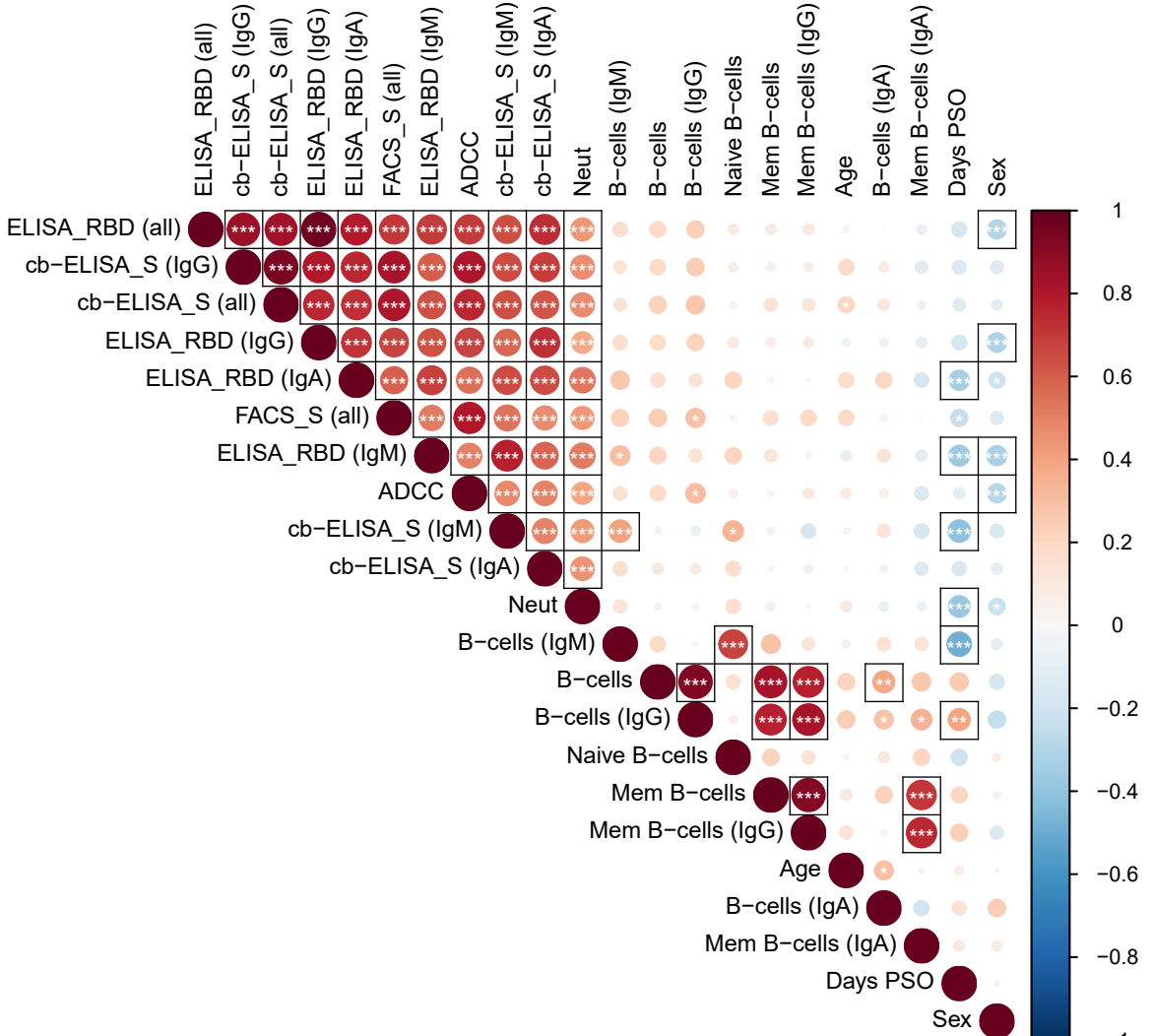

Supplemental Figure 5. Correlations between serological, immunological and demographic determinants - Related to Figure 5.

Correlograms were generated by plotting together all serological, immunological and demographic data obtained from convalescent patients. Circles are color-coded and sized according to the magnitude of the correlation coefficient (r). Red circles represent positive correlations between two variables and blue circles represent negative correlations. Asterisks indicate statistically significant correlations (*P < 0.05, **P < 0.01, ***P < 0.005). Correlation analysis was done using Spearman correlation rank tests. Parameters are clustered hierarchically according to the first principal component (FPC). Black surrounding boxes indicate adjusted p-values < 0.05 using Benjamini-Hochberg multiplicity correction. Legend: Cb-ELISA = cell-based ELISA, Neut = Neutralization, mem = memory, PSO =